

# Clinically Translatable Transcrocetin Delivery Platform for Correction of Tumor Hypoxia and Enhancement of Radiation Therapy Effects

Marie-Charlotte Diringer, Pierre Coliat, Clélia Mathieu, Nina Laurent, Carole Mura, Mainak Banerjee, Chen Zhu, Anna Grabowska, Alison Ritchie, Philip Clarke, Alexandre Bernard, Claire Vit, H el ene Burckel, Georges Noel, Peter Harvey, Xavier Pivot, and Alexandre Detappe\*

Improving the tumor reoxygenation to sensitize the tumor to radiation therapy is a cornerstone in radiation oncology. Here, the pre-clinical development of a clinically transferable liposomal formulation encapsulating trans sodium crocetinate (NP TSC) is reported to improve oxygen diffusion through the tumor environment. Early pharmacokinetic analysis of the clinical trial of this molecule performed on 37 patients orient to define the optimal fixed dosage to use in a triple-negative breast cancer model to validate the therapeutic combination of radiation therapy and NP TSC. Notably, it is reported that this formulation is non-toxic in both humans and mice at the defined fixed concentration, provides a normalization of the tumor vasculature within 72 h window after systemic injection, leads to a transient increase (50% improvement) in the tumor oxygenation, and significantly improves the efficacy of both mono-fractionated and fractionated radiation therapy treatment. Together, these findings support the introduction of a first-in-class therapeutic construct capable of tumor-specific reoxygenation without associated toxicities.

## 1. Introduction


Hypoxia is the hallmark of many tumors' malignancies, supporting carcinogenesis as well as resistance to radiation therapy and many other anticancer therapies.<sup>[1-3]</sup> In radiation oncology, the radiobiological effect of oxygen was one of the

first identified mechanisms related to the treatment activity.<sup>[4]</sup> Indeed, it was demonstrated that the killing of tumor cells by radiation in well-oxygenated regions is up to three times greater than in a hypoxic portion of the tumor. In addition, oxygen appears to be not only a sensitizer through chemical reactions, but also a trigger to some physiological and molecular effects in the tumor. Low oxygen levels within tumors result in hemodynamic changes and provoke neoangiogenic responses leading to leaky tumor vasculatures, limiting the transport of therapeutics into the tumor.<sup>[5-7]</sup>

As a result, many approaches to circumvent the therapeutic resistance induced by hypoxia have been examined through various clinical trials, such as the use of hyperbaric oxygen,<sup>[8]</sup> exogenous red blood cell transfusions,<sup>[9]</sup> systemic erythropoietin,<sup>[10]</sup> and nanoscale hemoglobin-based oxygen carriers (HBOCs)<sup>[11]</sup> that accumulate in the perivascular spaces of tumors by the enhanced permeability and retention (EPR) effect.<sup>[12,13]</sup> None of these approaches, however, have led to reliably successful clinical results to date,<sup>[14]</sup> with the exception of several antiangiogenic agents targeting the tumor vasculature

M.-C. Diringer, P. Coliat, C. Mathieu, N. Laurent, C. Mura, M. Banerjee, C. Zhu, A. Bernard, C. Vit, H. Burckel, G. Noel, X. Pivot, A. Detappe  
Institut de Canc erologie Strasbourg Europe  
Strasbourg, France  
E-mail: a.detappe@icans.eu

  2022 The Authors. Small published by Wiley-VCH GmbH. This is an open access article under the terms of the Creative Commons Attribution-NonCommercial License, which permits use, distribution and reproduction in any medium, provided the original work is properly cited and is not used for commercial purposes.

 The ORCID identification number(s) for the author(s) of this article can be found under <https://doi.org/10.1002/smll.202205961>.

DOI: 10.1002/smll.202205961

A. Grabowska, A. Ritchie, P. Clarke  
Ex Vivo Cancer Pharmacology Centre  
Biodiscovery Institute  
Translational Medical Sciences  
School of Medicine  
University of Nottingham  
UK

P. Harvey  
Sir Peter Mansfield Imaging Centre  
School of Medicine and School of Chemistry  
University of Nottingham  
UK

A. Detappe  
Strasbourg Drug Discovery and Development Institute (IMS)  
Strasbourg, France

either by preventing the formation of new blood vessels or by selectively damaging the abnormal blood vessels within tumors.<sup>[15–17]</sup>

Several studies have demonstrated that these agents could induce a normalization of the tumor vasculature, producing improvements in tumor perfusion and decreasing the interstitial pressure. The use of vascular-targeted agents to improve tumor oxygenation during radiotherapy and to increase the delivery and efficacy of anticancer drugs have offered great promise and substantial clinical benefits.<sup>[16]</sup>

However, given the limited efficacy and significant off-target toxicities observed with the aforementioned therapies, we focused our efforts on developing an approach that could improve the diffusion of oxygen within the deeper part of the tumor. Originally developed in patients with acute respiratory distress syndrome (ARDS) in the context of SARS-COV2,<sup>[18]</sup> the liposomal nanoparticles encapsulating trans sodium crocetin (NP TSC) demonstrated an improvement of the oxygen diffusion without associated toxicities; TSC is a kosmotropic agent enhancing systemic oxygen diffusion along a diffusion gradient in water and plasma based on its ability to alter the structure of water in plasma, causing additional hydrogen bonds to form in the water.<sup>[19–21]</sup> The encapsulation approach also enables the improvement of the circulation time of TSC in the blood to prolong its reported efficacy.<sup>[22–24]</sup> Currently being evaluated in Phase III clinical trial in ARDS, we sought to evaluate the NP TSC formulation in the context of cancer research to decrease the tumor hypoxia levels. In this context, we studied a triple negative breast cancer (TNBC) model; a tumor type well known for its high proliferation status providing extensive tumor growth with large hypoxic regions and active neoangiogenic development.

To advance this NP TSC formulation as a companion to external radiation therapy, we hypothesized that NP TSC would provide an adapted circulation time of the free TSC in the body i) to penetrate the tumor by EPR effect, and ii) to provide an adequate temporal window of reoxygenation within the tumor to enhance the efficacy of the external radiation therapy. The results presented here support the development of a therapeutic molecule that displays no toxicities at the defined fixed concentration, selective tumor uptake, and, when combined with localized radiation therapy, acts as a radiosensitizer by transiently reducing the amount of hypoxia levels within the core of the tumor to result in an enhanced radiation therapy effect.

## 2. Results and Discussion

### 2.1. Systemic Injection of a Fixed Dose of NP TSC Displays Minimal Off-target Toxicities in Mice and Humans

The NP TSC used in this study (Figure S1, Supporting Information) is currently being investigated in the context of COVID-19 as a reoxygenation molecule (Figure S2, Supporting Information). Thanks to this ongoing clinical trial (NCT04378920), we performed pharmacokinetic (PK) population modeling and simulation demonstrating that a fixed dose of NP TSC given every 12 h was comparable to a dose based on the patient's weight (i.e., 300 mg of encapsulated TSC, 2.62 g of phospholipids,

every 12 h versus an adjusted dosage of 2.5 mg kg<sup>-1</sup> of NP TSC every 24 h with or without an initial boost of 5 mg.kg<sup>-1</sup>). Indeed, the pharmacokinetic parameters of the fixed concentration (300 mg of NP TSC every 12 h) were within the margins of both dose-adjusted dosages and above the minimum threshold of activity in the blood that was preliminary determined as the target concentration to achieve (49 µg.mL<sup>-1</sup> of NP TSC), (Figure 1A–D, Figure S3, Supporting Information). As the fixed-dose PK profile was within the margins of error of the dose-adjusted approach, confirming the rationale to switch to this methodology of treatment, we, therefore, selected this concentration and dosing schedule to be used for this study.

However, the dose-limiting toxicity of the NP TSC formulation was linked to liver toxicities occurring at high doses in the phase I study. At the aforementioned recommended dose, no major toxicities directly linked to the systemic injection NP TSC were reported over 5 days of treatment, with the exception of transient toxicities in the liver (grade 3 hepatic biology increase; Figure S4, Supporting Information) inherent to the large quantities of administered liposomes. All the liver toxicities fully recovered at the interruption of the treatment.<sup>[25]</sup>

To repurpose this molecule as a companion drug for radiation therapy to act as a radiosensitizer, we translated these 300 mg fixed NP TSC doses to a pre-clinical concentration equal to ≈0.5 mg for a mouse (based on the abacus “mouse to human” provided by the US Food and Drug Administration (FDA)). The PK profile of the NP TSC was similar to those previously reported at lower concentrations of NP TSCs<sup>[18]</sup> (Figure 1E,F) for a single administration and confirmed the improvement of TSC circulation in the body in comparison to the free formulation (TSC only intravenous (i.v.) injection administered at the same concentration). At 0.5 mg, no acute nor chronic toxicities were observed in healthy nude mice after one i.v. injection per day for five consecutive days (Figure S5, Supporting Information), as well as no modification of their body weight (Figure S6, Supporting Information). These findings confirmed the safety profile of this NP TSC concentration at the pre-clinical level.

### 2.2. Cellular Morphologic Changes of Endothelial Cells and Their Permeability is Linked to the Reoxygenation Properties of NP TSC

Based on previously reported data for liposomes,<sup>[26,27]</sup> we expected ≈5% of the injected dose per gram (%ID/g) of the previously determined 0.5 mg of NP TSC to effectively reach the tumor. Using this previous data, we estimated the basal level of *in vitro* activity of the NP TSC should be observed at ≈25 µg mL<sup>-1</sup> of NP TSC (i.e., 76 µM of TSC). We first sought to validate the reoxygenation properties of the NP TSC on endothelial cells (HUVECs), as these cells would be the first impacted by the presence of NP TSC and free TSC in the tumor microenvironment. This decision is not only based on the usual passive targeting route used by liposomes to enter solid tumors, but also on the fact that the vast majority of NPs tend to penetrate the tumors through endothelial cells.<sup>[28]</sup>

We treated the HUVECs with various concentrations of NP TSC over 72 h to determine their toxicity (Figure 2A). The

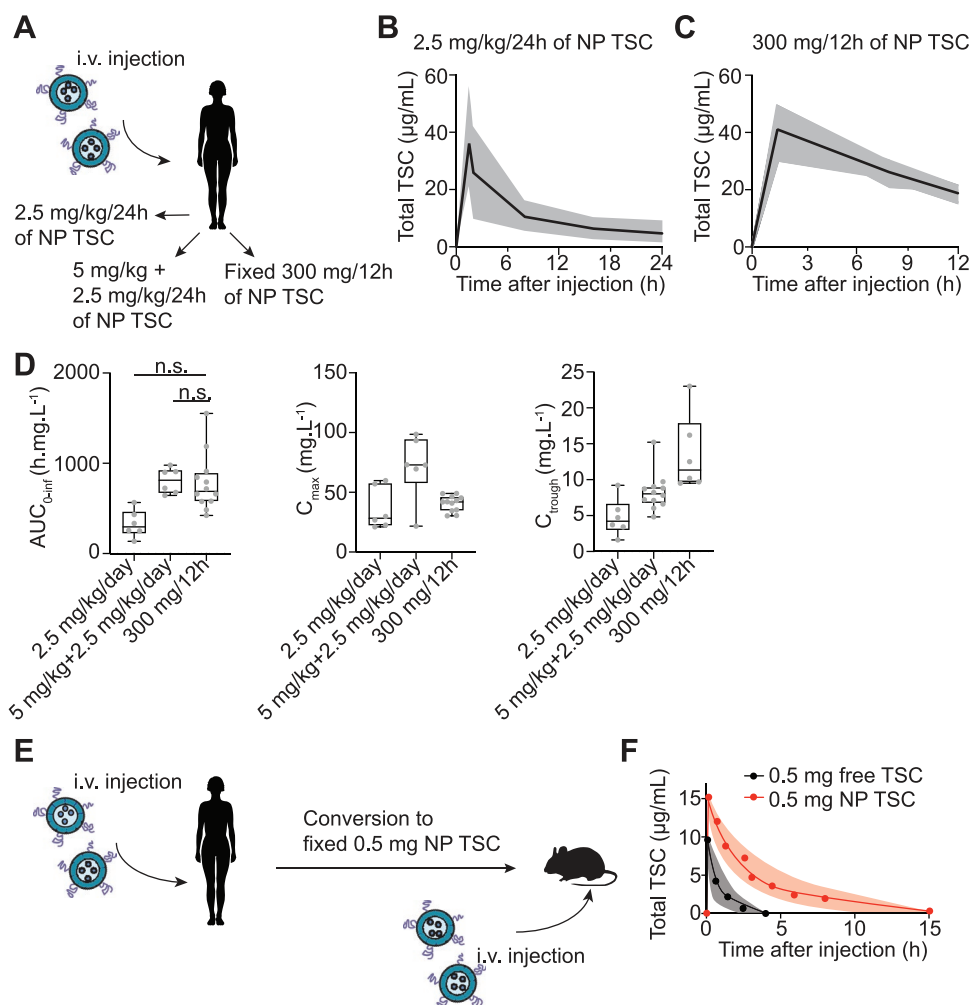


**Figure 1.** Determination of the pre-clinical fixed concentration of NP TSC based on preliminary clinical studies. A) Three cohorts (2.5 mg.kg<sup>-1</sup>/day, n = 6; 5 mg.kg<sup>-1</sup> + 2.5 mg.kg<sup>-1</sup>/day, n = 6; 300 mg/12 h n = 12) of patients were i.v. infused with NP TSC. B) Pharmacokinetic analysis was performed and analyzed over 24 h for the weight-adjusted NP TSC cohort (merged of the 2 cohorts without including the loading dose of 5 mg.kg<sup>-1</sup>) and C) fixed concentration NP TSC cohort. Data are represented as mean (solid line) ± std (grey area). D) Pharmacokinetic parameters confirmed that the fixed dose is within the margins of both dose-adjusted cohorts. *P*-value < 0.05, one-way ANOVA with post-hoc Bonferroni. E) The conversion of NP TSC concentration from human to mouse enabled to determine a fixed pre-clinical concentration of NP TSC equal to 0.5 mg of TSC. F) At this concentration, the NP formulation significantly improves the circulation time of the TSC in comparison to the free TSC i.v. administered at the same concentration. Data are represented as mean (solid line) ± std (shade).

observed IC<sub>10</sub> was calculated as ≈100 µg.mL<sup>-1</sup> and the IC<sub>50</sub> is equal to 218 µg.mL<sup>-1</sup> at 72 h post-treatment. To perform the reoxygenation studies, the HUVECs were cultivated overnight under normoxic (20% O<sub>2</sub>) or hypoxic (1% O<sub>2</sub>) conditions before treatment with various concentrations of NP TSC. An almost complete reoxygenation was observed after treatment under hypoxic conditions, with a plateau of reoxygenation (17% of PO<sub>2</sub>) observed from 50 µg.mL<sup>-1</sup> of NP TSC after 48 h of incubation (Figure 2B), which remains above the minimal targeted plasmatic concentration in humans (49 µg.mL<sup>-1</sup>).<sup>[18]</sup> As such, we selected 75 µg.mL<sup>-1</sup> of NP TSC as our baseline concentration for the remaining studies on the HUVECs to ensure a complete reoxygenation effect.

We further aimed to validate the impact of the reoxygenation properties of the NP TSC to aid in the permeabilization

of the endothelial cell layer. First, we identified that after 6, 24, and 48 h of treatment at 75 µg.mL<sup>-1</sup> of NP TSC, the size and the shape of the HUVECs did not differ from the untreated HUVECs under normoxic conditions. Interestingly, after 48 h of treatment with the NP TSC under hypoxic conditions, the size of the HUVECs tended to be similar to those in normoxic conditions and significantly larger than the untreated hypoxic control cells (Figure 2C). In addition, the HUVECs were more viable after 48 h of incubation in hypoxic conditions after being treated with NP TSC than without treatment (Figure S7, Supporting Information). This increase in the size of the HUVECs upon treatment with the NP TSC was also confirmed when we studied the permeability of the endothelial cell layer (Figure 2D). To validate the permeabilization of the endothelial cell layer, we treated them either in normoxic or hypoxic conditions using a

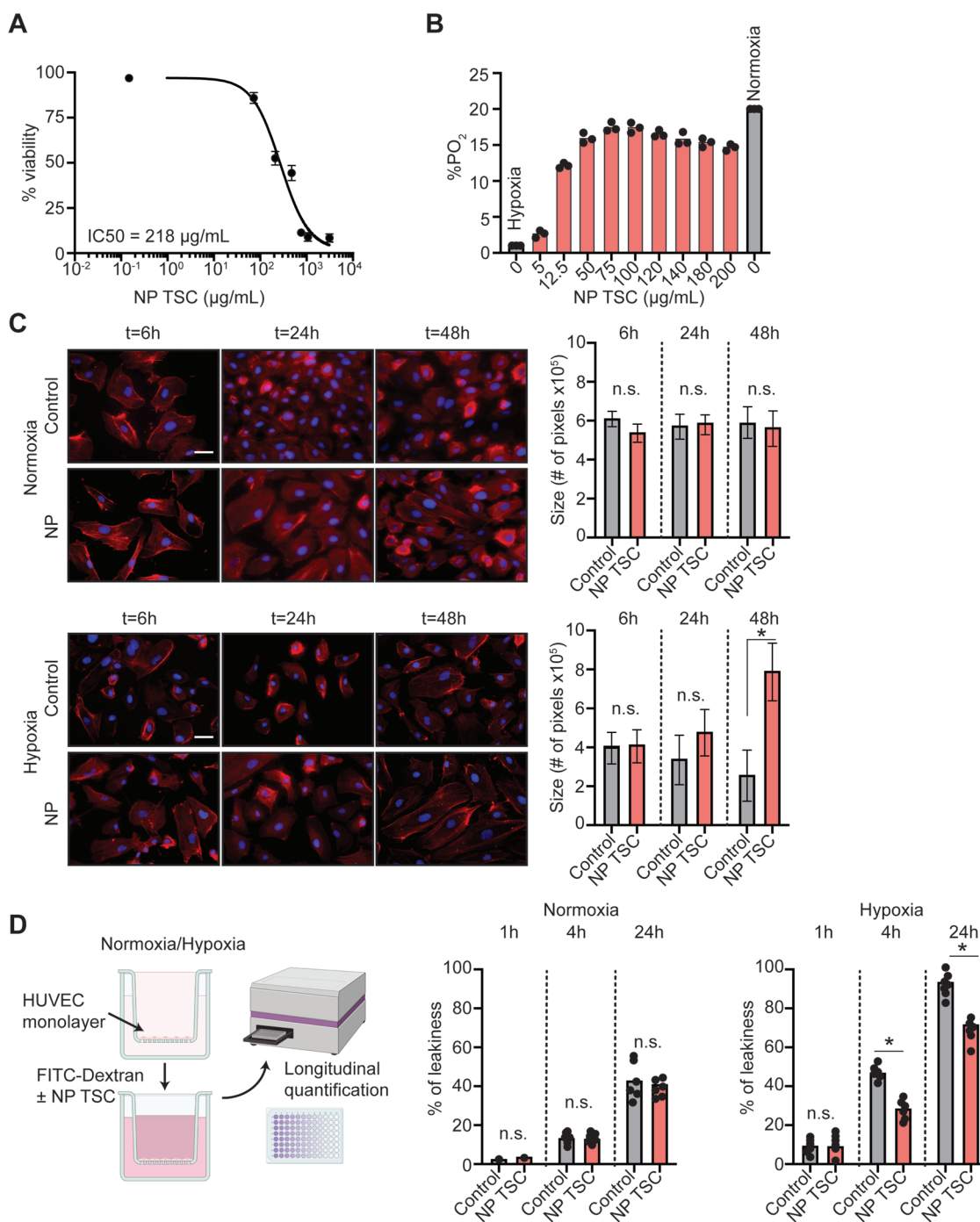


**Figure 2.** Reoxygenation of the endothelial cells (HUVECs) using NP TSC. A) The NP TSC is nontoxic to HUVECs with an IC<sub>10</sub> equal to ≈100 µg·mL<sup>-1</sup> at 72 post-treatments. B) A plateau of reoxygenation is observed from 50 µg·mL<sup>-1</sup>. C) NP TSC (75 µg·mL<sup>-1</sup>) allows the restoration of HUVECs under hypoxic conditions over time (n = 3 per condition). Magnification 40X, scale bar = 20 µm. Data are represented as mean ± std. D) The treatment of HUVECs with NP TSC (75 µg·mL<sup>-1</sup>) enables to decrease the endothelial permeability under hypoxic conditions (n = 3 per condition). Statistical analyses were performed using a two-tailed t-test, \* indicates a *p*-value <0.05.

well-chamber. FITC-dextran was then added on top of the cell layer and the total amount that leaked through the cell layer was quantified over time. While no differences in terms of FITC-dextran leakage was observed between non-treated and NP TSC-treated cells in normoxic condition, a significantly decreased amount of FITC-dextran was observed in hypoxic conditions

upon treatment with NP TSC, confirming the size increase of the HUVECs upon treatment leading to a decrease of the permeability of the endothelial layer with the NP TSC under hypoxic conditions. Altogether, these results suggest that the NP TSC has a direct effect on the endothelial cells under hypoxic conditions and tends to restore their morphological shape.



### 2.3. In Vitro Reoxygenation of Tumor Cells Enables Radiosensitization

We then evaluated the radiosensitization properties of the NP TSC on TNBC cells (MDA-MB-231). As observed with the HUVECs, we first validated that the NP TSC did not induce any toxicity to the cells (i.e., decrease of viability), with an  $IC_{50}$  in MDA-MB-231 cells calculated as  $485 \mu\text{g}\cdot\text{mL}^{-1}$  48 h after treatment (Figure 3A). Similarly to the HUVECs, we observed that the reoxygenation properties of the NP TSC are time- and concentration-dependent (Figure 3B), with the first signs of reoxygenation observed at  $\approx 24$  h post-treatment at high concentration ( $>160 \mu\text{g}\cdot\text{mL}^{-1}$ ), corresponding to the time at which the nanoparticles are internalized by the cells and exit the lysosomes.<sup>[29]</sup> Hence, subsequent in vitro radiosensitization studies were performed at  $75 \mu\text{g}\cdot\text{mL}^{-1}$  concentration to ensure full efficacy of the NP TSC was reached in vitro, with a treatment time of 24 h before external radiation therapy. Noteworthy, this concentration remains within the margins of toxicity observed by viability assay and in the same concentration range as for the HUVEC assays. We first validated the therapeutic efficacy of the combination radiation therapy-NP TSC in normoxic and hypoxic conditions by clonogenic assay (Figure 3C). Importantly, the reoxygenation effects induced by NP TSC in hypoxic conditions significantly increased the number of  $\gamma\text{H2AX}$  foci (a common biomarker of DNA double strand breaks) in cells in comparison to radiation therapy alone under the same culture conditions ( $p$ -value  $<0.001$  in both cell lines, t-test), confirming the benefit NP TSC could have in hypoxic tumors

(Figure 3D). To note, no differences were observed between the radiation group alone and the group combining NP TSC + radiation therapy in normoxic conditions, in contrast with the significant proliferation differences observed in hypoxic conditions favoring the exposure to NP TSC to radiosensitize the tumor cells. We then validated that the treatment of the cells with the NP TSC did not increase the basal level of  $\gamma\text{H2AX}$  foci in both normoxic and hypoxic conditions in MDA-MB-231 cells (Figure 3D). This experiment was further extended and validated to an additional cell type (A549) to confirm the versatility of the approach (Figures S8 and S9, Supporting Information).

### 2.4. A Decrease of Tumor Hypoxia Is Observed and Leads to Improve Radiation Therapy Efficacy

In the context of radiation therapy, we sought to reoxygenate the tumor through a single i.v. injection of NP TSC performed at the optimal peak of reoxygenation. In this context, we first observed the reoxygenation levels of the tumor after one i.v. injection (0.5 mg) of NP TSC. By using a xenograft tumor model of MDA-MB-231, we validated by fluorescence imaging that the NPs reach the tumor after  $\approx 4$  h post-injection and that the tumor retention is observed for at least 72 h. The mean tumor uptake is equal to  $3.3 \pm 1.2\% \text{ID/g}$  (Figure S10, Supporting Information), which is comparable to what can be achieved with other polymeric and lipidic NPs. Based on these results, we further analyzed *ex vivo* the tumor reoxygenation

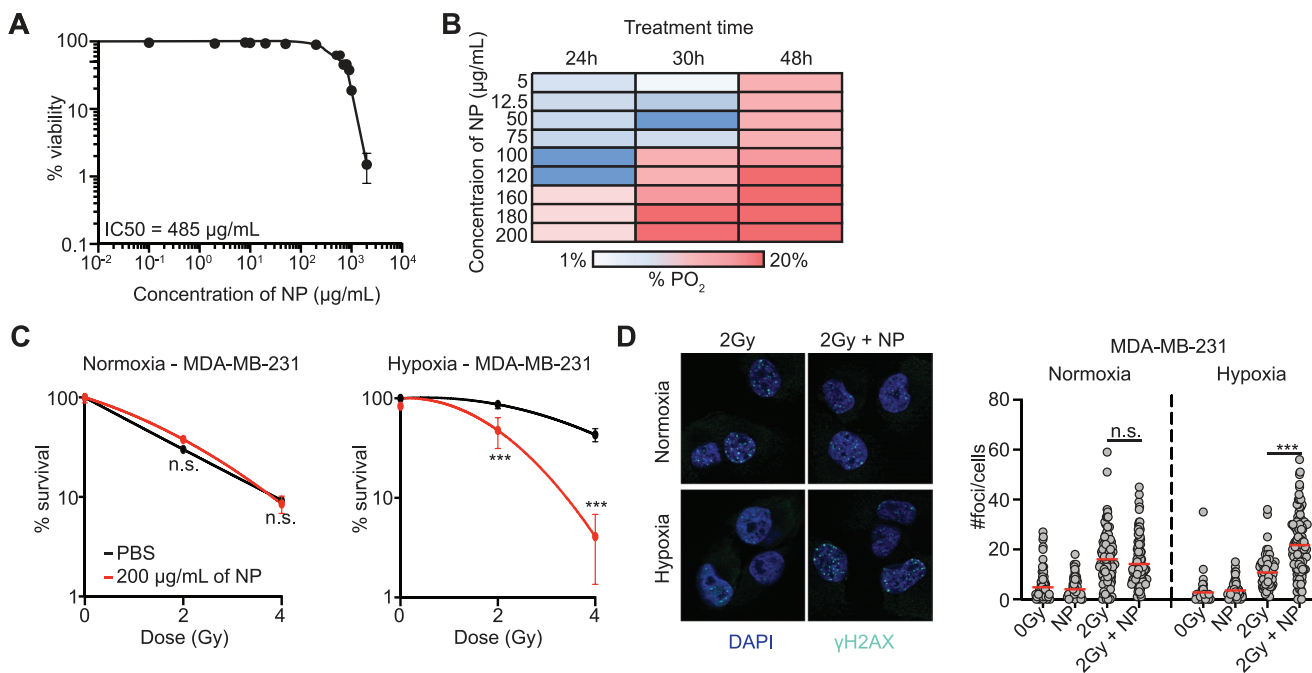


**Figure 3.** NP TSC enables the improvement of in vitro tumor radiosensitivity. A) NP TSC is non-toxic to MDA-MB-231 cells. B) Tumor cells (MDA-MB-231) reoxygenation is concentration dependent and persists over 48 h after treatment. C) Clonogenic assay confirms the radiosensitization effects of NP TSC ( $75 \mu\text{g}\cdot\text{mL}^{-1}$ ) in MDA-MB-231 cell line. Data are presented at mean  $\pm$  std. D) The DNA double-strand breaks are increased with the presence of  $75 \mu\text{g}\cdot\text{mL}^{-1}$  of NP TSC and 2 Gy irradiation under hypoxic conditions but do not modify the cell response in normoxic conditions in MDA-MB-231 cells. Red bar indicates the average value for each group. Statistical analyses were performed using a two-tailed t-test, \* indicates a  $p$ -value  $<0.05$ ,  $n = 3$  replicate per assay.

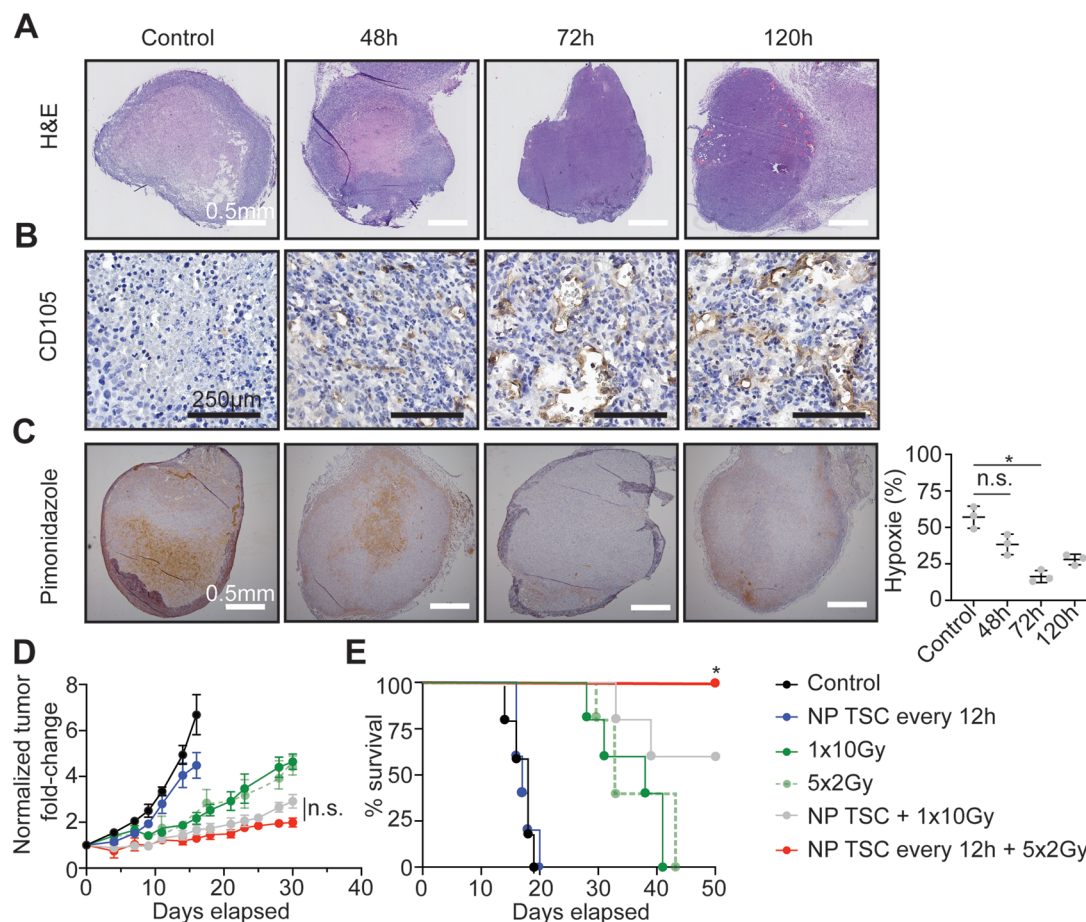


**Figure 4.** Therapeutic efficacy of NP TSC as a radiosensitizer in pre-clinical TNBC mouse model. A) Hematoxylin and eosin (H&E) staining of the tumors before, 48 h, and 72 h after treatment with 0.5 mg of NP TSC. B) CD105 staining confirming the increased amount of neovessels within the core of the tumor after treatment with NP TSC. C) Pimonidazole staining confirming the presence of hypoxia at randomization of the mice into the different tumor groups and the decrease levels 72 h after treatment with NP TSC. N = 3/group. D) Combined with radiation therapy (mono-fraction or fractionated treatment), the NP TSC demonstrates a synergistic effect and improves the tumor growth while E) enhancing the therapeutic benefit of external radiation therapy. In the context of mono-fraction, NP TSC was administered 72 h before radiation therapy. For the fractionated treatment, NP TSC was iv administered during the 5 days of treatment every 12 h, starting the evening before the first radiation treatment. N = 6/group. \* indicates a *p*-value <0.05, Log Rank test.

by performing hematoxylin and eosin staining (Figure 4A), CD105 staining to determine the effect of the NP TSC on the neovascularization of the tumor (Figure 4B, Figure S11, Supporting Information), and pimonidazole staining to quantify the hypoxia levels over time after a single i.v. injection of NP TSC (Figure 4C). The reoxygenation levels (i.e., decrease of the hypoxic staining) decreased over time with a maximal effect 72 h after treatment. This reoxygenation was, however, transient, as pimonidazole staining performed 120 h after treatment depicted clear hypoxic regions within the tumor margins. We hypothesized that this decrease of hypoxia within the tumors is induced by an improvement in the oxygen diffusion generated by the release of free TSC in the blood and tumors, leading to a normalization of the neovasculture architecture in the tumor.

Therefore, we next compared the effect of radiosensitization upon a single radiation dose (10 Gy) performed 72 h after treatment (maximal effect of reoxygenation). The injection of NP TSC without irradiation did not impact tumor growth or survival outcomes. However, once coupled to irradiation, NP

TSC treatment provided a significant improvement both in terms of tumor response (1.8-fold tumor growth inhibition compared to 10 Gy alone) (Figure 4D) and survival improvement (Figure 4E). Overall, treating the mice 48 h before irradiation provided the optimal therapeutic results (*p*-value <0.05, Log Rank test). Importantly, these treatments did not engender a loss of body weight in any of the studied groups (Figure S12, Supporting Information).

Based on the immunohistochemistry results, which suggest that i.v. injection of NP TSC 72 h before the first radiation treatment would be optimal (Figure 4A–C). We further aimed to validate the overall improvement of the therapeutic efficacy of the NP TSC in a more translationally-relevant radiation treatment. As such, instead of performing a  $1 \times 10$  Gy treatment, we performed a fractionated treatment of  $5 \times 2$  Gy with an i.v. maintenance of 0.5 mg of NP TSC every 12 h, starting 12 h before the initial fraction until the last radiation treatment (Figure 4D,E). Under these conditions, at day 50 after the irradiation dose, we observed a complete response with 100%

survival. Importantly, both groups treated with NP TSC combined with radiation therapy demonstrated a significant tumor growth inhibition in comparison to radiation therapy alone starting at 14 days after the inclusion in the study ( $p$ -value<0.05,  $t$ -test). Those results confirmed the potential therapeutic efficacy that provides NP TSC in combination therapy and its radiosensitivity properties.

### 3. Conclusion

While clinical data confirmed the tolerability of NP TSC and provided encouraging results in terms of overall patients reoxygenation in the context of severe COVID-19, this study enabled us to confirm pre-clinically the potential to restore normoxia transiently in hypoxic areas of the tumors to improve patient's tumor control using a fixed NP TSC dose. These data confirmed the possibility of transiently reoxygenating the tumor without impacting its tumor growth while providing a significant tumor radiosensitization effect, both under single high dose radiation therapy treatment or over a more conventional fractionated treatment with multiple administrations of NP TSC. These data suggest the need to further evaluate this molecule as a potential non-toxic radiosensitizer through clinical trials. This ability to correct hypoxia by increasing radiation therapy efficacy is a major indicator of the potential of NP TSC agent to improve the effectiveness of other anticancer agents impacted by the tumor hypoxic condition. In respect of TNBC, NP TSC might be combined with immunotherapy supporting a continued improvement of treatment.

### 4. Experimental Section

**Nanoparticle Synthesis:** NP TSC (also called LEAF-4L6715) was provided under good manufacturing process compliance by LEAF4Life (Woburn, MA). Briefly, NP TSC was prepared by the active loading of free transcroctin into liposomes through a calcium gradient.<sup>[8]</sup> HSPC, cholesterol, and DSPC-PEG<sub>2000</sub> were dissolved in chloroform (ratio 6:2:1), then multilamellar vesicles (MLVs) were formed by hydration of the lipids in calcium acetate solution at 65 °C (above HSPC transition temperature). The MLVs were passed through high-pressure extruder successively over 200 nm and then 100 nm polycarbonate membranes at 65 °C to form small unilamellar vesicles (SUVs). The external calcium acetate was removed by tangential flow filtration (TFF) to generate the calcium gradient. Free TSC was then mixed with the diafiltered liposomes and loaded into the liposomes through a heat exchanger. The TSC-loaded liposomes were purified by buffer exchange with histidine-buffered saline (pH 6.5, 10 mM histidine, 145 mM NaCl) through TFF. The bulk drug product was diluted to the target concentration of TSC (2 mg.mL<sup>-1</sup>), sterile filtered, and stored at 2–8 °C. The drug loading was 109 g.mol<sup>-1</sup> (drug/phospholids). The NP TSC drug products used in the clinical trial were manufactured in cGMP environment according to the procedures defined in the batch record and released after meeting the specifications. The average size of the NP-TSC was equal to 106 nm (DLS) with a polydispersity index of 0.133, and a charge equal to -10.2 mV at pH = 7.2.

**Cell Culture:** MDA-MB-231 cell line was purchased from ATCC (Manassas, VA, USA). MDA-MB-231 cells were cultivated in RPMI medium containing 10% fetal bovine serum, 1% penicillin/streptomycin. HUVECs were purchased from ATCC. The HUVECs were cultivated in ready to use endothelial cell growth medium (Sigma Aldrich, ref C-22010). A549 cell line was purchased from ATCC. A549 cells were

cultivated in Ham's F12 with L-glutamine medium containing 10% fetal bovine serum, 1% penicillin/streptomycin.

**Generation of Hypoxic Cells:** Cells were cultivated overnight under hypoxic conditions (1% O<sub>2</sub>, 5% CO<sub>2</sub>) using a cell incubator (InCu-saFe MCO-170 M, PHCHD). Cells were then treated with different conditions and stored back in the incubator for the length of the experiment.

**In vitro Studies—Viability assay:** HUVECs and MDA-MB-231 cells were plated at 5000 cells/well in a 96-well plate overnight and then treated for 72 h with varying concentrations of NP TSCs. Cell viability was determined by flow cytometry after Annexin V/Propidium Iodide staining following the manufacturer's instructions.

**Endothelial Morphology Experiment:** HUVECs were treated without or with 0.75 µg.mL<sup>-1</sup> of NP TSC under normoxic and hypoxic conditions. Cells were then fixed and stained with an anti-CD31 antibody to visualize the HUVEC membrane (anti-CD31-FITC, MiltenyiBiotech, ref 130-117-224) and DAPI (Fluoromont-G, ThermoFischer, ref 00-4959-52) before to be imaged by fluorescence microscopy (Nikon Eclipse 80i). The size of each cell was quantified using Fiji software by manual segmentation of 100 cells. The experiment was performed in triplicate.

**Quantification of the Cell Reoxygenation:** Cells (HUVEC and MDA-MB-231 cells) were treated with varying concentrations of NP TSC and incubated either under normoxic or hypoxic conditions. Over the course of treatment, 100,000 cells were stained with the BioTracker 520 Green Hypoxia dye (SigmaAldrich, #SCT033) for hypoxia quantification by flow cytometry (MACSQuant, MiltenyiBiotech). Data were normalized to untreated cells in normoxic conditions (20% O<sub>2</sub>) and hypoxic conditions (1% O<sub>2</sub>).

**Permeability Assay:** A total of 300,000 HUVECs were plated in transwell inserts fitting a 6-well plate overnight either under hypoxic or normoxic condition before being treated or not with NP TSC (0.75 µg.mL<sup>-1</sup>). We deposited on top of the tissue culture media 7.5 µL per well of CF488A-dextran 40 kDa (VWR, ref 80 126) at 2 mg.mL<sup>-1</sup>. The FITC-dextran solution leaking through the membrane was further quantified over time by a plate reader (ex/em 480/520 nm) (Molecular Devices, SpectraMax ID) to determine the permeability of the endothelial layer. Three experimental replicates were conducted that each contained 3 technical replicates per sample point. The concentration of FITC-dextran in each well was calculated based on its fluorescence emission using a standard curve.

**Clonogenic Assay:** A total of 5,000 cells of either MDA-MB-231 or A549 cells were plated in 6-well plates and incubated with 75 µg.mL<sup>-1</sup> of NP TSC for 24 h under normoxic or hypoxic conditions prior to irradiation with an open field 220 kVp beam. Radiation dose levels of 2, 4, 6, 8, and 10 Gy were employed using a Biobeam GM8000 machine (Gamma Service Medical). The cells were further incubated in hypoxic or normoxic conditions for an additional 5 days period post-radiation treatment before being washed, and stained with a 1% crystal violet in 10% ethanol dye solution. The plates were digitally scanned and manually counted. Measurements were performed in triplicate.

**In Vitro DNA Double-Strand Breaks:** MDA-MB-231 and A549 cells were incubated 24 h with NP TSC at a concentration of 75 µg.mL<sup>-1</sup> prior to 2 Gy irradiation. Cells were fixed in 4% paraformaldehyde in PBS at room temperature for 15 min. After fixation, cells were blocked in 1% BSA, 10% FBS, and 0.3% tritonX-100 in PBS. Next, cells were stained with anti-γH2AX antibody (Millipore) overnight at 4 °C. Subsequently, cells were incubated with secondary anti-mouse AlexaFluor-594 conjugated IgG (Abcam) for the noted primary antibody for 1 h at room temperature. A semi-quantitative analysis was performed to evaluate the number of foci per cell expressing the γH2Ax markers. Images were visualized with a Nikon Eclipse 80i microscope. Foci were identified in the images and their signal intensity was quantified using Fiji software.

**Statistical Analysis:** All in vitro and in vivo statistical analyses were performed with GraphPad Prism Software (V9.0).

**Animals:** All the animal procedures were performed in accordance with the Guidelines for Care and Use of Laboratory Animals as set forth by the Institutional Care and Use Committee (IACUC) of the Nottingham University.

**Preliminary Toxicity Evaluation of Fixed Dose of NP TSC:** Toxicity studies were performed in healthy female balb/c mice injected intravenously



every 12 h with 0.5 mg (in 200  $\mu$ L solution) of NP TSC for 1 week. Body weight was monitored daily, starting on the day of the first injection. After 20 days, the mice were sacrificed and blood samples were collected by heart puncture to determine basic metabolic profiles, complete blood counts, and white blood cell differential counts.

**Orthotopic Triple Negative Breast Cancer Model:** 750,000 MDA-MB-231<sub>Luc+</sub> cells were implanted in the mammary fat pad of the mice to generate the tumors. Tumor engraftment was assessed by bioluminescence imaging (IVIS, PerkinElmer). Mice were randomly attributed to a study group once the tumor reached 100 mm<sup>3</sup> in volume. The volume of the tumor was determined by daily caliper measurements. Mice were sacrificed when the tumor reached 1,500 mm<sup>3</sup>.

**Biodistribution Study:** Biodistribution studies were performed using fluorescently labeled NP TSC (Cy5.5) using the IVIS system. Mice were then sacrificed for *ex vivo* fluorescence quantification of the major organs ( $n = 3$ /time point).

**Proof-of-concept Study Confirming the Reoxygenation of the Tumors:** Injection of NP TSC at the pre-determined fixed concentration followed by sacrifice at 24, 48, and 72 h post treatment was performed. 90 min before euthanasia, intraperitoneal injection of 60 mg.kg<sup>-1</sup> of pimonidazole HCl (Hypoxyprobe Kit, Hypoxiprobe, Inc) 90 min prior to sacrifice. The NP TSC groups were culled at 24, 48, and 72 h post injection. *Ex vivo* staining was performed to stain the tumor as per the manufacturer protocol ( $n = 3$ /time point). After that, tumors were harvested and fixed for immunohistochemistry analysis.

**External Radiation Therapy Study:** Mice were irradiated using the Small Animal Radiation Research Platform (SARRP) (Xstrahl, Inc.). Animals were anaesthetized with 1–3% isoflurane for the duration of the irradiation. Similar to the clinical workflow, a cone beam computed tomography (CBCT) was performed on each mouse to calculate the dosimetry (Muriplan) and to determine the radiation beam arrangement (65 kVp, 1.5 mA). Treatment was performed using a 12 mm circular collimator (220 kVp, 13 mA). The radiation dose was delivered in one fraction of 10 Gy by two beams at 0° and 90° angles or in 5 fractions of 2 Gy using the same irradiation setup. A total of five mice per group were used to characterize the effect of the NP TSC as a radiosensitizer. In the NP TSC group, mice were *i.v.* administered 0.5 mg (200  $\mu$ L) of NP TSC. Each day, a caliper measurement was performed to determine the volume of the tumor.

*In vivo* experiments to investigate biodistribution and the effect of nanoparticles on reoxygenation were conducted under the UK Home Office Licence number PPL P435A9CF8. LASA good practice guidelines, FELASA working group on pain and distress guidelines, NCRI guidelines for the welfare and use of animals in cancer research, and ARRIVE reporting guidelines were also followed.

All mice were purchased from Charles River UK. Mice were maintained in individually ventilated cages (Tecniplast, UK) within a barrier unit, illuminated by fluorescent lights set to give a 12 h light-dark cycle (on 07.00, off 19.00), as recommended in the guidelines to the Home Office Animals (Scientific Procedures) Act 1986 (UK). The room was air-conditioned by a system designed to maintain an air temperature range of 21  $\pm$  2 °C and a humidity of 55%. Mice were housed in social groups, 4 per cage, during the study, with irradiated bedding and autoclaved nesting materials and environmental enrichment (Datesand UK). Sterile irradiated 5V5R rodent diet (IPS Ltd, UK) and irradiated water (Baxter, UK) were offered *ad libitum*. Mice were also weighed weekly and given a daily health check by an experienced technician.

After a week's acclimatisation, the mice were initiated with tumors. 40 female 6–8 week old CD-1 NuNu mice were implanted with  $2 \times 10^6$  MDA-MB231-HRE (MDA-MB231 cells expressing a hypoxia reporter, consisting of luciferase under the control of 3 hypoxia response elements and a minimal SV40 promoter in the pLVX [Clontech] backbone, introduced by lentiviral transduction) cells re-suspended in 100  $\mu$ L of Growth Factor Reduced Matrigel (Corning). Only female mice were used as the tumor under investigation was a breast line. Although only 32 mice were required for the study, 40 were set up in order to be able to select the 32 most evenly matched in terms of size. They were injected subcutaneously into the right-hand flank of the mice and the resulting tumors were measured twice weekly using Vernier calipers and

the volumes were calculated using the formula  $V = ab^2/6$ , where  $a$  is the length and  $b$  is the width. Tumors were also imaged weekly in the IVIS® Spectrum imaging system by 2D optical imaging, with tumor measurements made using Living Image (4.3.1) software and standard open filters to assess hypoxia levels based on the hypoxia reporter or the Hypoxisense probe (see below for details).

## 5. Biodistribution Study

The biodistribution study was performed as follows:

On day 43 after tumor initiation, when tumor volumes had reached an average of 200 mm<sup>3</sup>, 200  $\mu$ L of 5 mg.mL<sup>-1</sup> fluorescently labeled NP TSC (Cy5.5) were injected *i.v.* via the tail vein in 3 groups of three mice which were culled at 3 timepoints (4, 24, 48 h). Pimonidazole HCl (Hypoxyprobe Kit, Hypoxiprobe, Inc) at 60 mg.kg<sup>-1</sup> was injected intraperitoneally 90 min prior to sacrifice by an approved S1 method. *Ex vivo* fluorescent imaging of tumors and organs (kidney, urine (25  $\mu$ L), liver, spleen, pancreas, lung, heart, bladder, brain, lymph nodes-subiliac, spine, and whole blood (25  $\mu$ L)) was carried out using the IVIS Spectrum and data was analyzed using Living Image (4.3.1) software. The fourth group of three mice that did not receive nanoparticles was used as an imaging control. Tumors were fixed in 4% Neutral Buffered Formalin for immunohistochemistry analysis.

**Statistical Analysis:** All the data are presented as mean  $\pm$  std and all statistical analyses were performed with GraphPad Prism Software (V.8.1.0).

## Supporting Information

Supporting Information is available from the Wiley Online Library or from the author.

## Acknowledgements

A.D. acknowledges support from the Institut de Cancérologie Strasbourg Europe and the European Research Council (ERC) under the European Union's Horizon 2020 research and innovation program (ERC Starting Grant TheranolImmuno, grant agreement No. 950101). P.H. acknowledges support from a Nottingham Research Fellowship supported by the University of Nottingham. The authors also thank technical support for experiments conducted at the University of Nottingham from Marian Meakin (*in vivo*), Pam Collier and Catherine Probert (cells) and Sal Jones (histology), and from Pascal Kessler for the help at the PIC-STRA imaging platform from the University of Strasbourg.

## Conflict of Interest

The authors declare no conflict of interest.

## Author Contributions

A.D. and X.P. designed the research study. M.-C.D., N.L., C.M., P.C., C.M., V.M., M.B., A.G., A.R., P.C., P.H. performed the experiments. A.B., P.C., X.P., and A.D. analyzed the clinical trial data and toxicity studies. C.Z., H.B., G.N., X.P., and A.D. wrote the manuscript.

## Data Availability Statement

The data that support the findings of this study are available from the corresponding author upon reasonable request.



## Keywords

drug delivery, liposome, oxygenation, trans sodium crocetin

Received: September 28, 2022

Revised: December 8, 2022

Published online: January 1, 2023

- 
- [1] J. M. Brown, W. R. Wilson, *Nat. Rev. Cancer* **2004**, *4*, 437.  
[2] G. L. Semenza, *Cancer Cell* **2004**, *5*, 405.  
[3] W. R. Wilson, M. P. Hay, *Nat. Rev. Cancer* **2011**, *11*, 393.  
[4] L. H. Gray, A. D. Conger, M. Ebert, S. Hornsey, O. C. A. Scott, *Br. J. Radiol.* **1953**, *26*, 638.  
[5] R. K. Jain, *J. Clin. Oncol.* **2013**, *31*, 2205.  
[6] R. K. Jain, *Science* **2005**, *307*, 58.  
[7] M. A. Schneider, M. Linecker, R. Fritsch, U. J. Muehlemaier, D. Stocker, B. Pestalozzi, P. Samaras, A. Jetter, P. Kron, H. Petrowsky, C. Nicolau, J.-M. Lehn, B. Humar, R. Graf, P.-A. Clavien, P. Limani, *Nat. Commun.* **2021**, *12*, 3807.  
[8] P. M. Tibbles, J. S. Edelsberg, *N. Engl. J. Med.* **1996**, *334*, 1642.  
[9] L. T. Goodnough, M. E. Brecher, M. H. Kanter, J. P. AuBuchon, *N. Engl. J. Med.* **1999**, *340*, 438.  
[10] J. A. Glaspy, *Annu. Rev. Med.* **2009**, *60*, 181.  
[11] Z. Tao, P. P. Ghoroghchian, *Trends Biotechnol.* **2014**, *32*, 466.  
[12] Y. Shi, R. van der Meel, X. Chen, T. Lammers, *Theranostics* **2020**, *10*, 7921.  
[13] Y. Matsumura, H. Maeda, *Cancer Res.* **1986**, *46*, 6387.  
[14] S. Rey, L. Schito, M. Koritzinsky, B. G. Wouters, *Adv Drug Deliv Rev* **2017**, *109*, 45.  
[15] J. R. Mackey, R. S. Kerbel, K. A. Gelmon, D. M. McLeod, S. K. Chia, D. Rayson, S. Verma, L. L. Collins, A. H. G. Paterson, A. Robidoux, K. I. Pritchard, *Cancer Treat. Rev.* **2012**, *38*, 673.  
[16] R. Bell, J. Brown, M. Parmar, M. Toi, T. Suter, G. G. Steger, X. Pivot, J. Mackey, C. Jackisch, R. Dent, P. Hall, N. Xu, L. Morales, L. Provencher, R. Hegg, L. Vanlemmens, A. Kirsch, A. Schneeweiss, N. Masuda, F. Overkamp, D. Cameron, *Ann. Oncol.* **2017**, *28*, 754.  
[17] V. P. Chauhan, J. D. Martin, H. Liu, D. A. Lacorre, S. R. Jain, S. V. Kozin, T. Stylianopoulos, A. S. Mousa, X. Han, P. Adstamangkongkul, Z. Popovic, P. Huang, M. G. Bawendi, Y. Boucher, R. K. Jain, *Nat. Commun.* **2013**, *4*, 2516.  
[18] P.-M. Mertes, O. Collange, P. Coliat, M. Banerjee, M.-C. Diringier, A. Roche, X. Delabranche, V. Chaban, M. Voegelin, A. Bernard, V. Sartori, N. Laurent, M. Velten, N. Dhindsa, J. Defuria, G. Kim, Z. H. Xu, M. Theodorou, Z. R. Huang, K. Khalifa, B. Geng, C. Niyikiza, V. Moyo, P. Gizzi, P. Villa, A. Detappe, X. Pivot, *J. Controlled Release* **2021**, *336*, 252.  
[19] A. K. Stennett, G. L. Dempsey, J. L. Gainer, *J. Phys. Chem. B* **2006**, *110*, 18078.  
[20] J. Sheehan, J. Sherman, C. Cifarelli, J. Jagannathan, K. Dassoulas, C. Olson, J. Rainey, S. Han, *J. Neurosurg.* **2009**, *111*, 226.  
[21] J. Sheehan, A. Ionescu, N. Pouratian, D. K. Hamilton, D. Schlesinger, R. J. Oskoui Jr., C. Sansur, *J. Neurosurg.* **2008**, *108*, 972.  
[22] H. M. Shah, A. S. Jain, S. V. Joshi, P. S. Kharkar, *Drug Dev. Res.* **2021**, *82*, 883.  
[23] Z.-L. Guo, M.-X. Li, X.-L. Li, P. Wang, W.-G. Wang, W.-Z. Du, Z.-Q. Yang, S.-F. Chen, D. Wu, X.-Y. Tian, *Front. Pharmacol.* **2021**, *12*, 745683.  
[24] G. M. Holloway, J. L. Gainer, *J. Appl. Physiol.* **1988**, *65*, 683.  
[25] P.-M. Mertes, X. Delabranche, P. Coliat, A. Roche, O. Collange, M. Voegelin, A. Bernard, N. Dhindsa, Z. H. Xu, B. Geng, C. Niyikiza, V. Moyo, C. Bourban, P. Villa, A. Detappe, X. Pivot, medRxiv **2022**, 2022.09.07.22279668.  
[26] V. Mittelheisser, P. Coliat, E. Moeglin, L. Goepf, J. G. Goetz, L. J. Charbonniere, X. Pivot, A. Detappe, *Adv. Mater.* **2022**, *34*, 2110305.  
[27] S. Wilhelm, A. J. Tavares, Q. Dai, S. Ohta, J. Audet, H. F. Dvorak, W. C. W. Chan, *Nat. Rev. Mater.* **2016**, *1*, 16014.  
[28] S. Sindhwani, A. M. Syed, J. Ngai, B. R. Kingston, L. Maiorino, J. Rothschild, P. MacMillan, Y. Zhang, N. U. Rajesh, T. Hoang, J. L. Y. Wu, S. Wilhelm, A. Zilman, S. Gadde, A. Sulaiman, B. Ouyang, Z. Lin, L. Wang, M. Egeblad, W. C. W. Chan, *Nat. Mater.* **2020**, *19*, 566.  
[29] S. A. Smith, L. I. Selby, A. P. R. Johnston, G. K. Such, *Bioconjug Chem* **2019**, *30*, 263.